

The light-by-light contribution to the anomalous
magnetic moment of muon within the nonlocal chiral
quark models

Вклад от процесса рассеяния света-на-свете в
аномальный магнитный момент мюона в рамках
нелокальных кварковых моделей

A.E. Radzhabov^{a,1}, A.S. Zhevlakov^{a,b,2}

A.E. Раджабов^{a,1}, А.С. Жевлаков^{a,b,2}

^a Matrosov Institute for System Dynamics and Control Theory SB RAS, 664033,
Irkutsk, Russia

^a Институт динамики систем и теории управления имени В.М. Матросова СО
РАН, Иркутск

^b Joint Institute of Nuclear Research, BLTP, 141980, Moscow region, Dubna,
Russia

^b Объединенный институт ядерных исследований, Лаборатория
теоретической физики им. Н. Н. Боголюбова, Дубна

Представлен краткий обзор недавних расчетов адронного вклада от рассеяния света-на-света в аномальный магнитный момент мюона в нелокальной кварковой модели. В лидирующем порядке по $1/N_c$ этот вклад состоит из кварковой бокс-диаграммы, дополненной резонансными обменами. Ключевой особенностью данных расчетов является то, что двухфотонные форм-факторы мезонов в модели зависят не только от виртуальностей фотонов, но и от виртуальности самого мезона. Вследствие этого кварковая бокс-диаграмма обеспечивает правильную асимптотику операторного разложения. Показано, что результат модели остается достаточно стабильным при её расширении за счет включения частиц со спином 1.

A brief review of recent nonlocal quark model calculations of the hadronic light-by-light contribution to the muon's anomalous magnetic moment is presented. To the leading order in $1/N_c$, the contribution consists of a quark box diagram supplemented by resonance exchanges. A key point in these calculations is that the two-photon transition form factors of the mesons in the model depend not only on the photons' virtualities but also on that of the meson. Consequently, the quark box diagram provides the correct OPE asymptotic. It is shown that the model's result is quite stable when the model is extended to include spin-1 particles.

PACS: 12.39.Fe, 13.40.Em

¹E-mail: AERadzhabov@yandex.ru

²E-mail: zhevlakov1@gmail.com

¹E-mail: AERadzhabov@yandex.ru

²E-mail: zhevlakov1@gmail.com

Introduction

The anomalous magnetic moment (AMM) of the electron [1, 2] and the muon [3] are quantities that can be measured experimentally and calculated theoretically with high precision. The electron AMM is dominated by electromagnetic interactions, with only small corrections from strong interactions, whereas the muon AMM is more sensitive to other contributions. A discrepancy between the measured and calculated values could indicate the presence of unknown interactions – commonly referred to as New Physics (NP). For many years, the observed discrepancy made the muon AMM a promising signal for NP. However, the situation has changed dramatically in recent years.

The experimental measurement at Fermilab with a precision of 127 ppb [3] represents a fourfold improvement over the earlier result from Brookhaven National Laboratory [4].

On the theoretical side, while the electromagnetic and weak contributions are well-established and their precision has improved, the calculation of the strong interaction contribution is more challenging. The strong interaction contributions—hadronic vacuum polarization (HVP) and the subleading (in the fine-structure constant) hadronic light-by-light (LbL) scattering—cannot be reliably computed using perturbative QCD. For a long time, the leading-order HVP contribution was estimated primarily using experimental data on e^+e^- annihilation into hadrons. However, recent cross-section measurements of $e^+e^- \rightarrow \pi^+\pi^-$ from the threshold up to 1.2 GeV by the CMD-3 collaboration [5] deviate significantly from all previous results. Conversely, a lattice QCD calculation by the BMW Collaboration [6] achieved sub-percent precision for the HVP contribution, comparable to the precision of the data-driven methods. Consequently, the White Paper (WP) 2025 [7] employs the lattice QCD value for the Standard Model prediction of the muon AMM. As a result, the discrepancy between the latest experimental result [3] and the WP 2025 update [7] has substantially diminished, indicating no significant tension between experiment and theory within the current precision.

The aim of this work is to present the results of our recent papers [8, 9], which calculate the LbL contribution within a nonlocal quark model that includes vector and axial-vector particles, and to compare them with the results obtained in the model with only scalar and pseudoscalar sectors [10–12].

Quark models

The Lagrangian of the $SU(2)$ model, which incorporates pseudoscalar, scalar, vector, and axial-vector mesons, is given by

$$\mathcal{L} = \mathcal{L}_{free} + \mathcal{L}_{P,S} + \mathcal{L}_{V,A}, \quad \mathcal{L}_{free} = \bar{q}(x)(i\hat{\partial} - M_c)q(x), \quad (1)$$

$$\mathcal{L}_{P,S} = \frac{G_1}{2} \left(\left(J_S^a(x) \right)^2 + \left(J_P^a(x) \right)^2 \right), \mathcal{L}_{V,A} = \frac{G_2}{2} \left(\left(J_V^{a,\mu}(x) \right)^2 + \left(J_A^{a,\mu}(x) \right)^2 \right),$$

where M_c is the current quark mass matrix with diagonal elements m_c , while G_1 and G_2 are the coupling constants in the pseudoscalar–scalar (P,S) and vector–axial–vector (V,A) sectors, respectively. For the strange quark sector, a straightforward generalization of the four-quark interactions to the $SU(3)$ group is insufficient. To correctly describe the η – η' mass splitting, the six-quark 't Hooft determinant interaction must also be included in the Lagrangian

$$\mathcal{L} = \mathcal{L}_{free} + \mathcal{L}_{P,S} - \frac{H}{4} T_{abc} [J_S^a(x) J_S^b(x) J_S^c(x) - 3 J_P^a(x) J_P^b(x) J_P^c(x)]. \quad (2)$$

where H is six-quark coupling constant.

The nonlocal quark currents are given by

$$J_M^{a\{\cdot,\mu\}}(x) = \int d^4x_1 d^4x_2 f(x_1) f(x_2) \bar{q}(x - x_1) \Gamma_M^{a\{\cdot,\mu\}} q(x + x_2), \quad (3)$$

with $M = S, P, V, A$. The spin-flavor matrices are defined as: $\Gamma_S^a = \lambda^a$, $\Gamma_P^a = i\gamma^5 \lambda^a$, $\Gamma_V^{a,\mu} = \gamma^\mu \lambda^a$, $\Gamma_A^{a,\mu} = \gamma^5 \gamma^\mu \lambda^a$. In the $SU(2)$ case, the flavor matrices are given by $\lambda^a \equiv \tau^a$ for $a = 0, \dots, 3$, where $\tau^0 = \mathbf{1}$. This interaction structure finds motivation in the instanton liquid model [13]. The function $f(x)$ represents a form factor encoding the nonlocal nature of the QCD vacuum. The $SU(2)$ model can be bosonized via the standard Hubbard–Stratonovich transformation by introducing auxiliary mesonic fields P, S, V, A for each quark bilinear. For the $SU(3)$ case, however, the bosonization requires the use of the stationary phase approximation [14].

The scalar isoscalar field develops a nonzero vacuum expectation value, $\langle S^0 \rangle_0 = \sigma_0 \neq 0$. Shifting the field as $S^0 = \tilde{S}^0 + \sigma_0$ to obtain a physical scalar field with zero vacuum expectation value leads to the emergence of a momentum-dependent quark mass. The separable structure of the quark current allows the momentum dependence to be factorized, resulting in a gap equation of simple form. For the $SU(2)$ model, it reads:

$$m(p) = m_c + m_d f^2(p), \quad m_d = G_1 \frac{8N_c}{(2\pi)^4} \int d^4k \frac{f^2(k^2) m(k^2)}{k^2 + m^2(k^2)}. \quad (4)$$

This gap equation for the scalar coefficient m_d can be solved numerically. The corresponding quark propagator is given by

$$S(p) = (\hat{p} - m(p))^{-1}. \quad (5)$$

Meson propagators are derived from the quadratic terms in the meson fields in the one-loop effective Lagrangian. The quark loops contributing to the propagators of vector and axial-vector mesons must be decomposed into longitudinal and transverse components with the help of appropriate projectors. The transverse components correspond to physical spin-1 states, while the

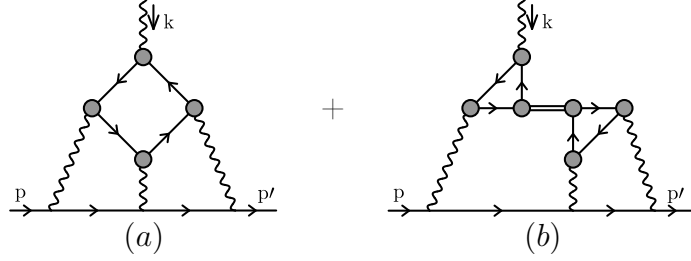


Fig. 1. Leading-order $1/N_c$ topologies for the hadronic light-by-light contribution: (a) quark box diagram; (b) meson resonance exchanges.

longitudinal components are related to spin-0 degrees of freedom. In the case of coupled pseudoscalar–axial-vector states, mixing arises through quark polarization loops involving both pseudoscalar and axial-vector vertices. The physical states of the π – a_1 system are determined by solving the matrix equation. Interactions with the electromagnetic gauge field are incorporated into the nonlocal quark currents, which generates additional nonlocal vertices involving an arbitrary number of photons [12]. Furthermore, the photon acquires dressing through intermediate vector mesons. This dressing does not lead to renormalization of the photon mass or quark charge, as required by electromagnetic gauge invariance [9].

LbL contribution

The projection technique can be used to calculate the LbL contribution to the muon's AMM:

$$\begin{aligned}
 a_\mu^{\text{HLbL}} &= \frac{1}{48m_\mu} \text{Tr}((\hat{p} + m_\mu)[\gamma^\rho, \gamma^\sigma](\hat{p} + m_\mu)\Pi_{\rho\sigma}(p, p)), \\
 \Pi_{\rho\sigma}(p', p) &= -ie^6 \int \frac{d^4 q_1}{(2\pi)^4} \int \frac{d^4 q_2}{(2\pi)^4} \frac{1}{q_1^2 q_2^2 (q_1 + q_2 - k)^2} \gamma^\mu \times \\
 &\times \frac{\hat{p}' - \hat{q}_1 + m_\mu}{(p' - q_1)^2 - m_\mu^2} \gamma^\nu \frac{\hat{p} - \hat{q}_1 - \hat{q}_2 + m_\mu}{(p - q_1 - q_2)^2 - m_\mu^2} \gamma^\lambda \frac{\partial}{\partial k^\rho} \Pi_{\mu\nu\lambda\sigma}(q_1, q_2, k - q_1 - q_2),
 \end{aligned} \tag{6}$$

where m_μ is the muon mass, and the static limit $k_\mu \equiv (p' - p)_\mu \rightarrow 0$ is implied. By averaging over the direction of the muon momentum, the result for a_μ^{HLbL} becomes a three-dimensional integral with the radial integration variables Q_1, Q_2 and the angular variable [12].

In order to obtain the diagrams contributing to the LbL process in the quark model, it is necessary to use $1/N_c$ counting rules: each quark loop yields a factor of N_c due to the trace over color indices, while each meson propagator contributes a factor of $1/N_c$. Therefore, at leading order in $1/N_c$, the LbL amplitude is saturated by two topologies of diagrams, schematically depicted in Fig. 1: the quark box (a) and resonance exchanges (b). In the model, the transition form factor depends not only on the virtualities of the photons but

also on that of the meson. This dependence arises because mesons are quark-antiquark bound states. A similar situation occurs in the local NJL model and in the Dyson-Schwinger approach to QCD. This dependence leads to a suppression of the resonance exchange contributions shown in Fig. 1(b). As a result, the correct QCD asymptotic behavior is provided by the box diagram contribution [10], while resonance exchanges and vector-meson dressing of photons do not alter this result [9]. In the model, the transition form factor depends not only on the virtualities of the photons but also on that of the meson. This dependence arises because mesons are quark-antiquark bound states. A similar situation occurs in the local NJL model and in the Dyson-Schwinger approach to QCD. This dependence leads to a suppression of the resonance exchange contributions shown in Fig. 1(b). As a result, the correct QCD asymptotic behavior is provided by the box diagram contribution [10], while resonance exchanges and vector-meson dressing of photons do not alter this result [9].

The LbL contribution in the model with spin-1 particles differs from that in the model without the vector meson sector for the following reasons:

- The model parameters differ, as they are fitted to observables including π - a_1 mixing,
- There is an additional intermediate axial-vector LbL contribution of the type shown in Fig. 1(b),
- The internal photon lines are dressed by intermediate vector meson exchanges.

The total LbL contribution in the model with only scalar-pseudoscalar degrees of freedom is $(168 \pm 12.5) \times 10^{-11}$ [12]. The estimated contribution in the model with vector-axial-vector sector is¹ [9]

$$a_\mu^{\text{HLbL}} = (154 \pm 12.4) \times 10^{-11}. \quad (7)$$

A comparison of our results with spin-1 particles [8,9] and the model with only scalar-pseudoscalar interactions [10–12] is presented in Fig. 2, alongside results from lattice QCD, phenomenological estimates, effective models², Dyson-Schwinger studies, and AdS/QCD calculations. Additionally, we show the difference between the experimental value [3] and the theoretical prediction from the WP 2025 update [7] without the HLbL contribution. When combining our LbL result (7) with the WP 2020 values [15], a significant theory-experiment discrepancy of approximately 200×10^{-11} persists. However, using the WP 2025 values [7] together with our LbL contribution (7) not only changes the sign of the discrepancy but also reduces its magnitude to about -1×10^{-11} . Thus, our result substantially constrains the

¹The strange-quark sector contribution is taken from the model without spin-1 mesons.

²The line between effective models and phenomenological approaches is somewhat blurred.

parameter space for NP scenarios while producing a theoretical value consistent with experimental measurements of the muon's anomalous magnetic moment.

Acknowledgement

The authors thank the A.P. Martynenko, F.A. Martynenko and V.P. Lomov for fruitful comments. AER thanks the Organizing Committee of the XXVIth International Baldin Seminar on High Energy Physics Problems for the opportunity to present this report.

Funding

This work is supported by the project of the Ministry of Education and Science of the Russian Federation (“Analytical and numerical methods of mathematical physics in problems of tomography, quantum field theory, fluid and gas mechanics” no. 121041300058-1).

Conflict of interest

The authors of this work declare that they have no conflict of interest.

REFERENCES

1. *Fan X., Myers T.G., Sukra B.A.D., Gabrielse G.* // Phys. Rev. Lett. 2023. V. 130, no. 7. P. 071801. arXiv:2209.13084.
2. *Hanneke D., Fogwell S., Gabrielse G.* // Phys. Rev. Lett. 2008. V. 100. P. 120801. arXiv:0801.1134 [physics.atom-ph].
3. *Aguillard D.P. et al.* [Muon g-2] // Phys. Rev. Lett. 2025. Jun. V. 135, no. 10. P. 101802. arXiv:2506.03069.
4. *Bennett G.W. et al.* [Muon g-2] // Phys. Rev. D. 2006. V. 73. P. 072003.
5. *Ignatov F.V. et al.* [CMD-3] // Phys. Rev. D. 2024. V. 109, no. 11. P. 112002. arXiv:2302.08834.
6. *Borsanyi S. et al.* // Nature. 2021. Feb. V. 593, no. 7857. P. 51–55.
7. *Aliberti R. et al.* // Phys. Rept. 1143 (2025) 1-158. 2025. May. V. 1143. P. 1–158. arXiv:2505.21476.
8. *Radzhabov A.E., Zhevlakov A.S., Martynenko A.P., Martynenko F.A.* Phys. Rev. D. 2023. V. 108, no. 1. P. 014033. arXiv:2301.12641.
9. *Radzhabov A.E., Zhevlakov A.S.* // Phys. Rev. D. 2025. V. 112. P. 094008.

10. *Dorokhov A.E., Radzhabov A.E., Zhevlakov A.S.* // Eur. Phys. J. C. 2011. V. 71. P. 1702. arXiv:1103.2042 [hep-ph].
11. *Dorokhov A.E., Radzhabov A.E., Zhevlakov A.S.* // Eur. Phys. J. C. 2012. V. 72. P. 2227. arXiv:1204.3729 [hep-ph].
12. *Dorokhov A.E., Radzhabov A.E., Zhevlakov A.S.* // Eur. Phys. J. C. 2015. V. 75, no. 9. P. 417. arXiv:1502.04487.
13. *Anikin I.V., Dorokhov A.E., Tomio L.* // Phys. Part. Nucl. 2000. V. 31. P. 509–537.
14. *Reinhardt H., Alkofer R.* // Phys. Lett.B. 1988. V. 207. P. 482–488.
15. *Aoyama T. et al.* // Phys. Rept. 2020. V. 887. P. 1–166. arXiv:2006.04822.
16. *Chao E.H., Hudspith R.J., Gérardin A., Green J.R., Meyer H.B.* // Eur. Phys. J. C. 2022. aug. V. 82, no. 8. P. 664. arXiv:2204.08844.
17. *Blum T. et al.* [RBC, UKQCD] // Phys. Rev. D. 2023. 4. V. 111, no. 1. P. 014501. arXiv:2304.04423.
18. *Fodor Z., Gerardin A., Lellouch L., Szabo K.K., Toth B.C., Zimmermann C.* // Phys. Rev. D. 2025. Nov.. V. 111, no. 11. P. 114509.
19. *Hoferichter M., Stoffer P., Zillinger M.* // Phys. Rev. Lett. 2025. Feb. V. 134, no. 6. P. 061902. arXiv:2412.00190.
20. *Danilkin I., Redmer C.F., Vanderhaeghen M.* // Prog. Part. Nucl. Phys. 2019. V. 107. P. 20–68. arXiv:1901.10346.
21. *Jegerlehner F.* The Anomalous Magnetic Moment of the Muon. Cham : Springer, 2017. V. 274. P. 1–693.
22. *Prades J., de Rafael E., Vainshtein A.* // Adv. Ser. Direct. High Energy Phys. 2009. V. 20. P. 303–317. arXiv:0901.0306 [hep-ph].
23. *Jegerlehner F., Nyffeler A.* // Phys. Rept. 2009. V. 477. P. 1–110.
24. *Bijnens J., Pallante E., Prades J.* // Nucl. Phys.B. 2002. V. 626. P. 410–411.
25. *Hayakawa M., Kinoshita T.* // arXiv:hep-ph/0112102v2.
26. *Greynat D., de Rafael E.* // JHEP. 2012. jul. V. 2012, no. 7. P. 020.
27. *Goecke T., Fischer C.S., Williams R.* // Phys. Rev. D. 2013. V. 87, no. 3. P. 034013. arXiv:1210.1759 [hep-ph].
28. *Leutgeb J., Mager J., Rebhan A.* // Phys. Rev. D. 2025. Nov.. V. 111, no. 11. P. 114001. arXiv:2411.10432.

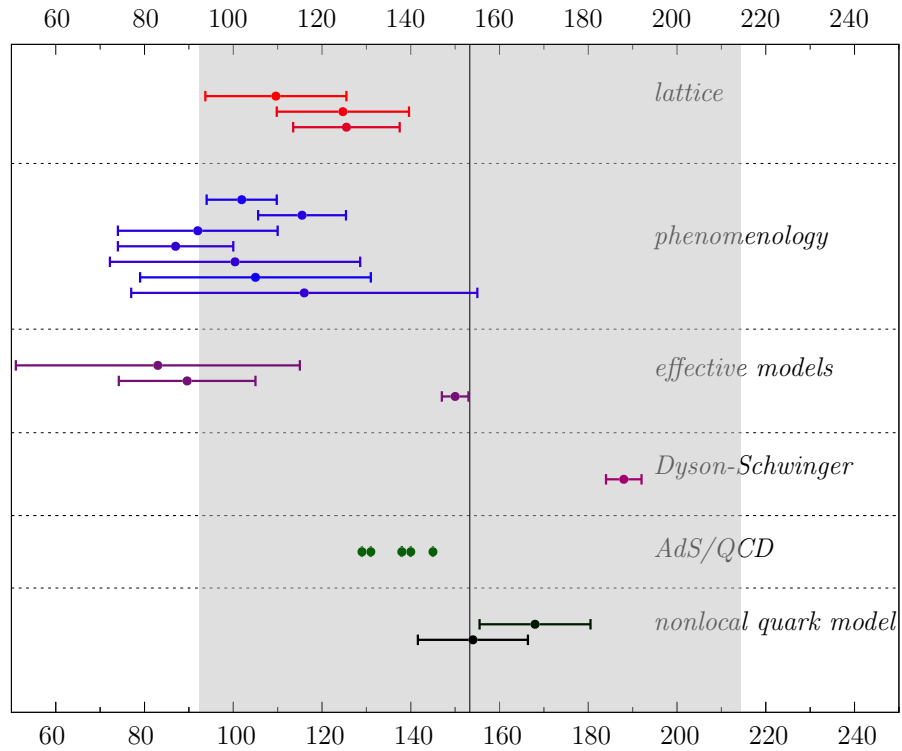


Fig. 2. Hadronic LbL contribution in different approaches (references given from top to bottom): lattice QCD calculations (Mainz) [16], (RBC/UKQCD) [17], (BMWc) [18]; phenomenological estimations in dispersive formalism HSZ2025 [19], using combinations of different contributions WP 2025 [7], WP 2020 [15], DRV2019 [20], J2017 [21], “Glasgow consensus” [22], N/JN2009 [23]; in effective models ENJL+ $\pi(K)$ loop (BPP) [24], ENJL+HLS + phenomenology (HKS) [25], in C_χ QM [26]; DSE&BSE studies GFW2013 [27]; AdS/QCD result for different models LMR2024 [28]; in nonlocal quark model without vector and axial-vector mesons [12] and with spin-1 particles [9]. The thin vertical line corresponds to difference between experimental value [3] and theoretical prediction minus HLbL contribution while shaded region to the theoretical error without HLbL contribution from WP 2025 [7].